Available online at www.sciencedirect.com
ScienceDirect
European Polymer Journal 43 (2007) 762–772
EUROPEAN POLYMER JOURNAL
www.elsevier.com/locate/europolj

Macromolecular Nanotechnology

Surface initiated ATRP in the synthesis of iron oxide/polystyrene core/shell nanoparticles

Yabin Sun [a,b], Xiaobin Ding [a,*], Zhaohui Zheng [a], Xu Cheng [a], Xinhua Hu [a], Yuxing Peng [a,*]

[a] *Chengdu Institute of Organic Chemistry, Chinese Academy of Sciences, Chengdu 610041, PR China*
[b] *Graduate School of the Chinese Academy of Sciences, Beijing 100081, PR China*

Received 26 June 2006; received in revised form 20 October 2006; accepted 21 October 2006
Available online 21 December 2006

Abstract

A method to prepare magnetic nanoparticles with a covalently bonded polystyrene shell by surface initiated atom transfer radical polymerization (ATRP) was reported. First, the initiator for ATRP was covalently bonded onto the surface of magnetic nanoparticles through our novel method, which was the combination of ligand exchange reaction and condensation of triethoxysilane having an ATRP initiating site, 2-bromo-2-methyl-*N*-(3-(triethoxysilyl)propyl) propanamide. Then the surface initiated ATRP of styrene mediated by a copper complex was carried out and exhibited the characteristics of a controlled/"living" polymerization. The as-synthesized nanoparticles were coated with well-defined PS of a target molecular weight up to 45 K. These hybrid nanoparticles had an exceptionally good dispersibility in organic solvents and were subjected to detailed characterization using DLS, GPC, FTIR, XPS, UV–vis, TEM and TGA.

Keywords: Polymer composite materials; Atom transfer radical polymerization; Magnetic nanoparticles

1. Introduction

As a result of anisotropic dipolar attraction, pristine nanoparticles of iron oxides tend to aggregate into large clusters and thus lose the specific properties associated with single-domain, magnetic nanostructures. Therefore, surface modification of magnetic nanoparticles (MNPs) is an essential and challenging step for most of their applications and fundamental studies. Polymeric shells have some unique advantages because of the flexibility in the controls of chemical compositions and functions of the polymers. Among many approaches for coating the surface of nanoparticles with a shell of organic polymers, the surface initiated atom transfer radical polymerization (ATRP) has become a method of choice recently [1]. Several groups have reported the synthesis of the polymeric core/shell nanoparticles such as SiO_2 [2], Au [3], $MnFe_2O_4$ [4], and Fe_2O_3 [5] via ATRP. ATRP can offer polymeric shells with low polydispersity and this method is easy to control the molecular weight, thereby, the thickness of the polymeric shell [6].

* Corresponding authors. Tel.: +86 028 85233426; fax: +86 028 85233426.
E-mail address: lgsyb@hotmail.com (Y. Peng).

0014-3057/$ - see front matter
doi:10.1016/j.eurpolymj.2006.10.021

However, as far as we know, previous ATRP studies for the synthesis of core/shell MNPs usually yield a carboxylates bonded shell of polymeric molecules protecting iron oxide cores. The linear polymeric molecules attach to the surface of iron oxide cores through the initiator via the –COOH group. For instance, Wang et al. [5] has utilized a solvent-free ATRP approach for the synthesis of the core/shell nanoparticles in which iron oxide cores are protected with a layer of carboxylates bonded polystyrene shell. A simple carboxylates linkage between the iron oxide core and the polymeric chain is not sufficient to achieve a permanent linkage. Instead, a dynamic exchange between the polymeric chains and other competing molecules possessing a –COOH group can lead to the dissociation of the polymeric chains from the core surfaces. To solve the problem, Li et al. [7] use divinylbenzene (DVB) as a crosslinker copolymerized with styrene through ATRP. But the disadvantage of this method is that the introduction of DVB into the polymerization mixture leads to the crosslinking among particles.

Recently, some groups have reported the trialkyloxysilane or trichlorosilane with initiating site for ATRP to be covalently bonded on the surface of MNPs through sol–gel method [8]. However, most of them can not avoid any silica encapsulated small aggregates of several MNPs due to the trialkoxysilane or trichlorosilane's high trend to self-condensation.

In the present paper, we would like to report our synthesis of the iron oxide/polystyrene core/shell nanoparticles via surface initiated ATRP. First our novel method was employed to covalently bond initiators onto the surface of MNPs, which was the combination of ligands exchange reaction and condensation of triethoxysilane having an ATRP initiating site, 2-bromo-2-methyl-*N*-(3-(triethoxysilyl) propyl) propanamide [9]. Then the polystyrene shell was grafted from the initiating sites on the surface of MNPs through ATRP. The covalently bonded polymeric shell could prevent the undesired site exchange of the MNPs surface functionalities.

2. Experimental section

2.1. Materials

Ferrous sulfate heptahydrate, ferric chloride hexahydrate, oleic acid (OA), 2-bromoisobutyryl bromide, γ-aminopropyl triethoxysilane (APS), copper bromide (CuBr, 99.0%), *N*,*N*,*N*′*N*″,*N*″-pentamethyldiethylenetriamine (PMDETA) were purchased from Aldrich Chemical Co. and used as received. Styrene was washed with aqueous NaOH to remove inhibitors, then dried for several hours with $MgSO_4$ and distilled under reduced pressure. Toluene was purified by distillation from CaH_2. Triethylamine (TEA) was dried over potassium hydroxide and distilled from CaH_2 before use. All other reagents were used as received from commercial sources.

2.2. Synthesis of OA coated MNPs

OA coated MNPs were synthesized via a two-step method (Scheme 1). First step: 2.35 g ferrous sulfate heptahydrate ($FeSO_47H_2O > 99\%$) and 4.1 g ferric chloride hexahydrate ($FeCl_36H_2O > 99\%$) were dissolved into 100 mL deionized water in a flask. This solution was stirred, followed by adding 25 mL 25% (w/w) NH_3H_2O quickly at room temperature. The solution color changed from orange to black, leading to a black precipitate. Then under vigorous stirring, 1 mL OA was dropped into the dispersion slowly at 80 °C in 1 h. The whole process was carried out under nitrogen atmosphere. The as-synthesized MNPs could be well dispersed into water by the protection of the double layers of OA.

Second step was to extract MNPs from water into toluene. In a typical procedure, 50 mL MNPs' water dispersion and 50 mL toluene were mixed together in a 250 mL extractor. By adding small amount of sodium chloride, MNPs transferred into toluene phase and under the protection of single layer of OA, they had good dispersibility in toluene. Finally, the toluene dispersion was refluxed to remove most of the water under nitrogen atmosphere and the content of MNPs was diluted with toluene to 10 mg/mL.

2.3. Synthesis of 2-bromo-2-methyl-N-(3-(triethoxysilyl)propyl) propanamide (BTPAm)

BTPAm was synthesized as follows: toluene (10 mL) with 2-bromoisobutyryl bromide (0.1 mL, 0.8 mmol) was added dropwise to a cold solution of γ-aminopropyl triethoxysilane (APS) (0.18 mL, 0.8 mmol) in dry toluene (10 mL) with TEA (0.12 mL, 0.8 mmol) at 0 °C. The mixture was magnetically stirred for 3 h at 0 °C and then for another

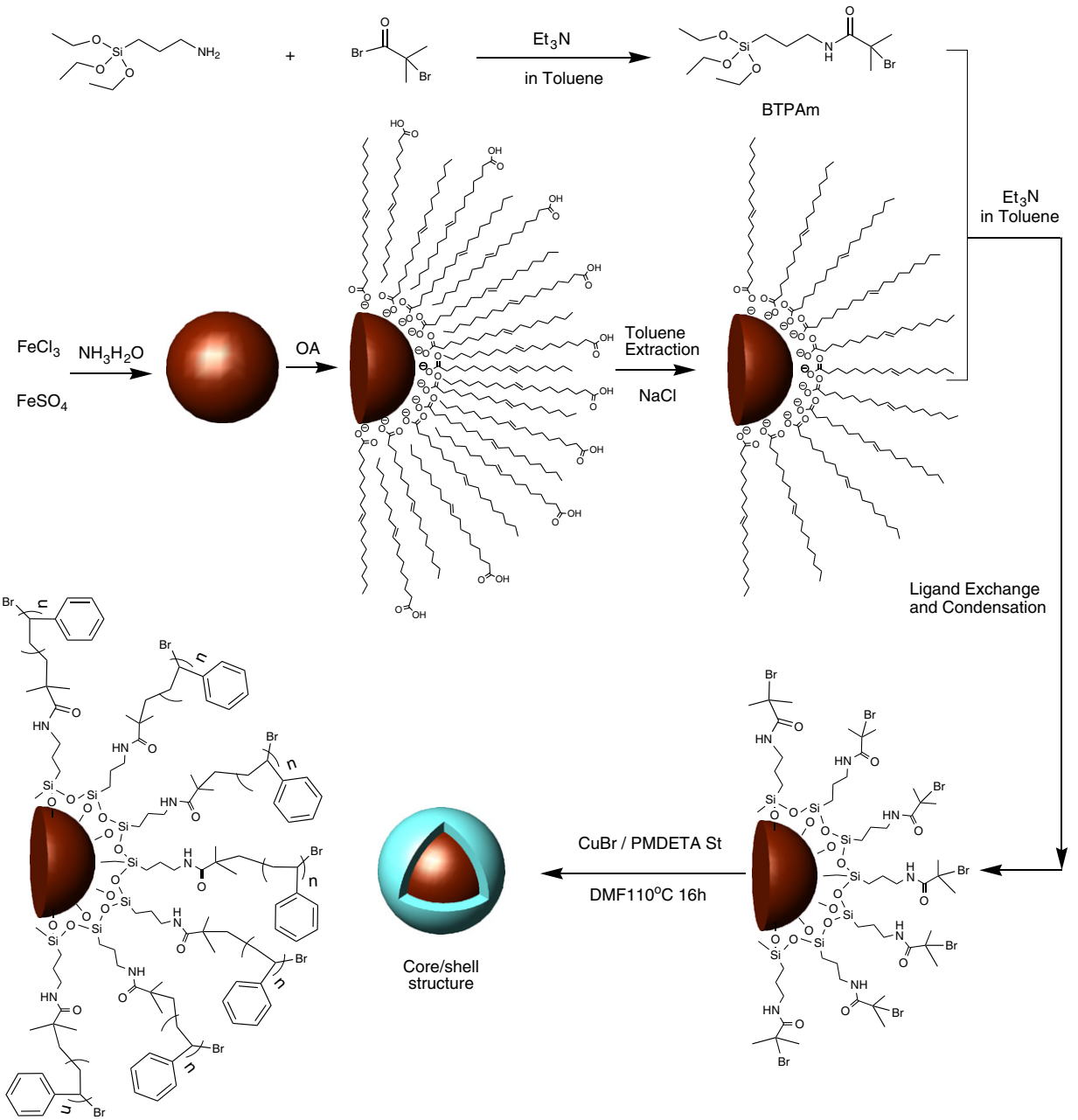

Scheme 1. Illustration of the synthesis route of polystyrene coated MNPs with core/shell structure.

10 h at room temperature. The mixture was passed through a filter paper to remove the salts and the filtrate was evaporated to remove the unreacted TEA under reduced pressure. ^{1}H-NMR ($CDCl_3$): 0.58 (t, 2H, SiCH_2), 1.17(t, 9H, CH_3CH_2OSi), 1.58(m, 2H, CH_2), 1.82(q, 6H, CH_3C), 3.15 (t, 2H, CH_2NH), 3.7 (t, 6H, CH_3CH_2OSi), 6.85(s, 1H, N*H*).

2.4. Synthesis of initiator-coated MNPs

The initiator-coated MNPs were synthesized as follows: First, 0.05 mL BTPAm, 1 mL TEA (2 M in toluene), 10 mL toluene and 5 mL toluene based MNPs dispersion were added into a 50 mL round-bottom flask. The mixture was stirred for 48 h at room temperature under nitrogen atmosphere. Sec-

ondly, 20 mL petroleum ether was added into the mixture to precipitate the modified MNPs, followed by magnetic separation and dried in vacuum. Thirdly, these MNPs were re-dispersed into toluene and re-precipitated by petroleum ether. This procedure was repeated 5 times to remove the ungrafted initiators and replaced OA followed by dried in vacuum. Finally, MNPs were dispersed into styrene with content of 0.01 g/mL.

2.5. Surface initiated ATRP on MNPs

First, to a 10 mL Schlenk flask, Cu(I)Br (28.8 mg, 0.2 mmol), PMDETA (0.042 mL, 0.2 mmol) and 0.5 mL DMF were added, and the atmosphere was exchanged for N_2. The mixture was stirred until the homogenous blue color was seen. Next, 4 mL styrene based initiator-coated MNPs dispersion was added via syringe. The flask was immediately degassed by three freeze-pump-thaw cycles with N_2, and then the mixture was stirred in a constant temperature oil bath at 110 °C for 16 h; 0.20 mL samples were removed with a purged syringe at desired intervals to estimate monomer conversion and for GPC measurement to determine molecular weight and its distribution. The viscosity of the solution increased with time. After the polymerization was complete, the remaining polymerization solution was diluted with THF and added to CH_3OH, and a brown solid precipitated. The solids were isolated by an external magnetic filed and volatile materials were removed in vacuum. PS chains were cleaved from the MNPs as follows: the polymer-grafted MNPs (0.1 g) were decomposed with HF aqueous solution and then neutralized. Organic polymers were extracted with THF and chloroform and dried under vacuum, and then subjected to GPC measurement.

2.6. Measurements

Transmission electron microscopy (TEM) was carried out on a JEM-100CX instrument operating an acceleration voltage of 80 kV. TEM specimens were prepared by aspirating an toluene based dispersion sample onto a copper EM grid.

A UV–vis spectrometer (VARIAN cary 100 Con, USA) was used to measure the absorption of the core/shell nanoparticles solution in a quartz cell.

Infrared spectrums were recorded by a Nicolet 200SXV-1 FT–IR spectrometer with KBr.

The hydrodynamic diameters and distribution of the MNPs of were measured with a Zetasizer Nano ZS90.

X-ray photoelectron spectroscopy (XPS) was carried out on an XSAM-800 electron and take-off angle of 20° was used with X-ray source.

XRD data were collected on a Shimadzu XD-D1. X-ray diffractometer employing Cu Kα radiation at 30 kV and 30 mA.

Number average molecular weights (M_n), weight average molecular weight (M_w), and molecular weight distribution (M_w/M_n) were determined using gel permeation chromatography (GPC) in THF at 30 °C with a flow rate of 1 mL min^{-1}.

Thermogravimetric analysis (TGA) was performed on a TA instrument Q50, at a scan rate of 10 °C min^{-1}, up to 800 °C under nitrogen atmosphere.

The number of initiator molecules grafted onto the surface of MNPs was calculated from elemental analysis and TGA, respectively. And the graft density of PS was calculated only from TGA analysis. The graft density of OA, BTPAm and PS were calculated from TGA analysis and their molecular weight according to the following equation:

$$\text{No. of molecules per nm}^2 = \frac{W \times d_{Fe_3O_4} \times r \times N_A}{M(1-W) \times 3 \times 10^{21}},$$

where W is the weight loss of sample, d_{Fe_3O4} is the density of Fe_3O_4, N_A is Avogadro's constant, M is the molelcule weight, r is the radius of MNPs.

3. Result and discussion

3.1. Synthesis of the OA coated MNPs

The synthesis strategy was designed and presented in Scheme 1. First, a stable colloidal dispersion of MNPs was prepared by co-precipitation method using OA as surfactants. MNPs were extracted into toluene only by adding some salts as inducer, such as NaCl, KCl, KI, NaBr etc., which was similar with the nanosized silver colloids [10]. XRD analysis indicates that magnetite (Fe_3O_4) is the resulting material. The XRD pattern (Fig. 1) of MNPs is similar to the ASTM XRD graphics of Fe_3O_4. The experimental d-spacings from X-ray patterns are 3.00, 2.52, 2.09, 1.61, and 1.48 at characteristic peaks of 2-Θ, 29.72, 35.57, 43.17, 57.15 and 62.77, respectively, which is very similar to ASTM

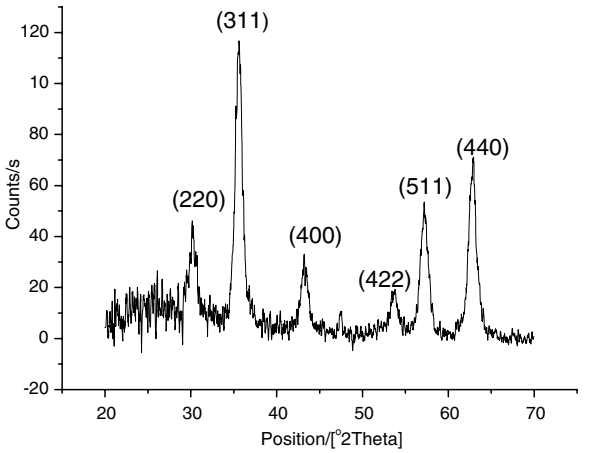

Fig. 1. X-ray powder diffraction patterns of the Fe_3O_4 nanoparticles.

data for iron oxide (d (Fe_3O_4)), 2.97, 2.53, 2.10, 1.62 and 1.48.

The size of MNPs calculated by analyzing XRD peaks using the integral-breath method is 9 nm, which is similar to 9.1 nm determined by DLS and 9 nm by TEM. The consistent between TEM and DLS analysis indicates that MNPs can be well dispersed in toluene.

FT–IR analysis was performed to determine the surface composition of the resulting MNPs, as depicted in Fig. 2a. The spectrum shows characteristic absorption bands of OA on the MNPs surface. The 1560 cm^{-1} and 1450 cm^{-1} bands belong to the presence of coordinated COO^- groups of OA with Fe_3O_4, which confirm the bonding of the OA ligand to the surface of MNPs through COO^- functionality. Similar results of the COO^- group band were also observed for OA adsorbed on cobalt nanoparticles [11] and Fe_2O_3 nanoparticles [5]. The 594 cm^{-1} and 622 cm^{-1} bands belong to Fe_3O_4, which are highly consistent with the spectrum of magnetite. The C=O stretching frequency of OA ligand at 1706 cm^{-1} is also observed in the spectrum, which suggests the presence of "free" OA in the dispersion. To further determine the surface chemical composition of MNPs, XPS analysis was carried out. The photoelectron lines at binding energy of about 53 eV, 284 eV, 530 eV, and 710 eV, which are attributed to Fe3p, C1s, O1s, and Fe2p, respectively, are observed in the wide scan spectrum of the OA coated MNPs (Fig. 3a). The content of Fe on the surface is only 4%, indicating that MNPs are well covered with OA layer. Two peak components are observed in their C1s core-level spectrum. The peak at about 284.6 eV is attributed to C–C and C–H, and the peak at 288.7 eV is attributed to COOH. The area ratio of the two peaks is 16.8:1, which is close to the theoretical ratio of 17:1 for OA (Fig. 4b), also confirming the OA layer on the MNPs.

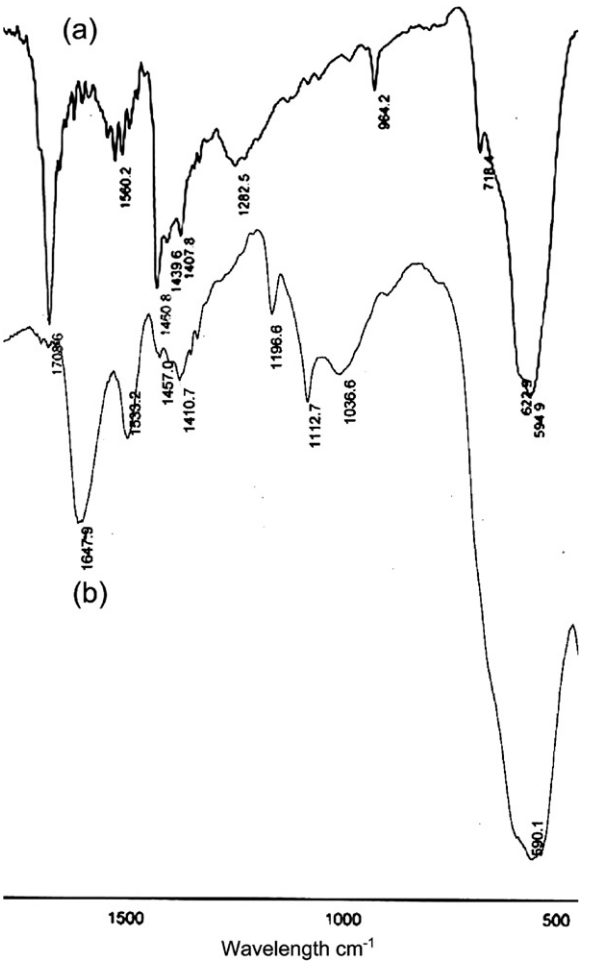

Fig. 2. IR spectrums of the MNPs: (a) OA coated and (b) BTPAm modified.

3.2. Synthesis of BTPAm

It is well established that trialkoxysilane molecules hydrolyze, oligomerize, and finally condense with hydroxyl groups present at the surface of oxide particles [12]. Many groups have synthesized the mono- or trichlorosilane derivatives, the monoethoxysilane or triethoxysilane derivative. For instance, Ohno et al. have synthesized the triethoxysilane derivative through a two steps method [2]. The first: 5-hexen-1-ol was acylated with 2-bromoisobutyryl

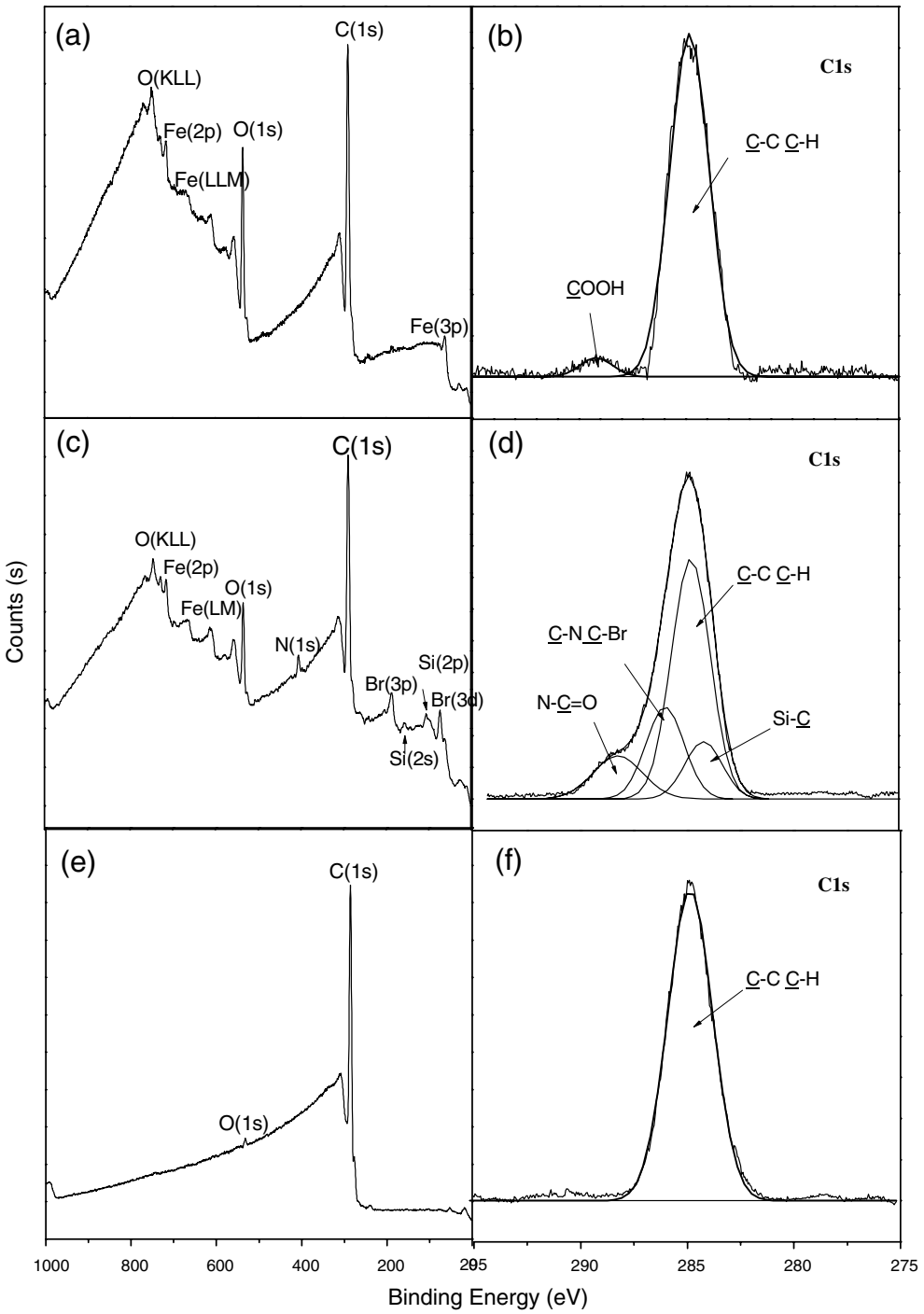

Fig. 3. XPS of MNPs: (a) and (b) OA coated; (c) and (d) BTPAm modified; (e) and (f) PS coated.

bromide to obtain (2-bromo-2-methyl)propionyloxyhexyl-triethoxysilane (BHE). The second: the aryl group of BPH was subsequently hydrosilylated with triethoxysilane in the presence of Karstedt's catalyst to give the final product (2-bromo-2-methyl)propionyloxyhexyl-triethoxysilane (BHE). Obviously, its disadvantage is the longer synthetic route. Here, we used one step method to synthesize BTPAm, which was the reaction between γ-aminopropyl triethoxysilane and

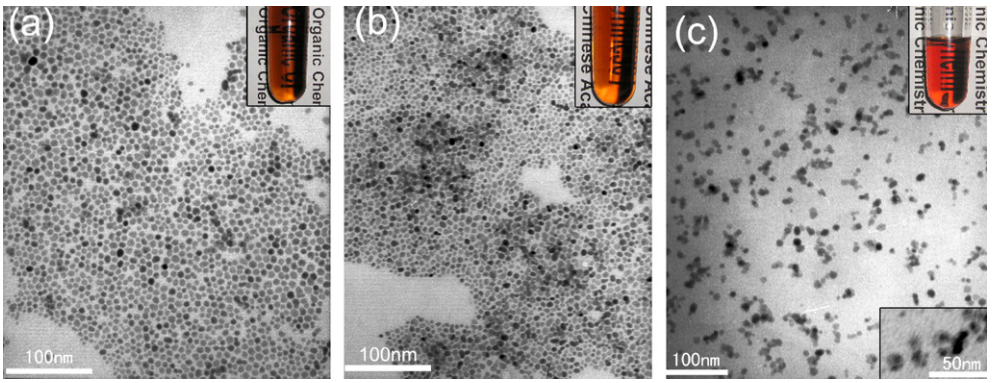

Fig. 4. TEM images of magnetic nanoparticles: (a) OA coated in toluene; (b) BTPAm modified in St and (c) PS coated in toluene.

2-bromoisobutyryl bromide. The structure of BTPAm was confirmed by ^{1}H-NMR.

3.3. Immobilization of initiators on MNPs

As far as we know, the sol–gel method, which is often used in the modification of nanoparticles, is difficult to control to avoid any silica encapsulated small aggregates of several MNPs due to the trialkoxysilane' high trend to self-condensation [13]. Recently, ligand exchange reaction has been proved to be an effective way to modify the surface of nanoparticles without any aggregates [14]. However, the disadvantage of this method is the carboxylates bonds between ligand and the surface of MNPs. A simple carboxylates linkage between the iron oxide core and the polymeric chain is not sufficient to achieve a permanent linkage. Instead, a dynamic exchange between the polymeric chains and other competing molecules possessing a –COOH group can lead to the dissociation of the polymeric chains from the core surface. We have developed a novel approach in the immobilization of initiator for ATRP, which is the combination of ligand exchange reaction and condensation of triethoxysilane. It takes the advantages of these two methods: covalent linkage between initiator and surface of MNPs and no aggregates formed during the modification. TEM pictures of MNPs before and after modification of BTPAm are given in Fig. 4a and b, which indicate that the morphology of MNPs almost maintains their original state.

FT–IR and XPS were carried out to analyze the chemical composition of the surface of BTPAm modified MNPs. As shown in Fig. 2b, after BTPAm modification, the N–C=O bond presents at 1647 cm^{-1} and 1533 cm^{-1}. The large band around 1000 cm^{-1} corresponds to Si–O–Si vibrations and attests to the formation of a silica layer that entraps one MNP. XPS analysis in Fig. 3c confirms the immobilization of initiator on the surface of MNPs. The characteristic signals for silicon (Si2s at 155 eV and Si2p at 103 eV), nitrogen (N1s at 403 eV), and carbon (C1s at 285 eV) and (Br3p at 184 eV and Br3d at 72 eV) are clearly observed in the wide scan spectrum and the molar ratio of the carbon/silicon/Br is 6.9/0.9/1, which is close to the theoretical ratio of 7:1:1 for BTPAm. Four peaks are observed in the C1s core-level spectrum of the BTPAm modified MNPs (Fig. 3d). The peak at about 284.8 eV is attributed to *C*–C and *C*–H, the peak at 288.3 eV is attributed to N–*C*=O, the peak at 283.4 eV is attributed to Si–*C* and the peak at 286 eV is attributed to N–*C* and *C*–Br. The area ratio of the four peaks is 2.9/1/0.9/2, which is close to the theoretical ratio of 3/1/1/2 for BTPAm. The appearance of the C–Si and C–Br species, as well as the N–*C*=O, confirms the presence of initiators on MNPs surface. Both FT–IR and XPS analysis show us that OA that absorbed on MNPs has been replaced by BTPAm completely.

In this reaction, a catalyst, such as TEA and pyridine, was required. Replaced OA was bonded with TEA or pyridine through the COO^- functionality, which accelerated the procedure of ligands exchange between OA and BTPAm. In addition, TEA or pyridine could catalyze the hydrolyzation of triethoxysilane to silanol. Besides catalyst, water also played an important role. Reflux was necessary to remove the most of "free" water that was not absorbed on the surface of MNPs, but existed in the micelle formed by "free" OA in toluene. More "free" water resulted in the triethoxysilane hydrolyzing outside of the surface of MNPs and

condensed with each other, which led to the formation of silica encapsulated small aggregates of MNPs. It was suggested that the surface of MNPs was the main place where the triethoxysilane groups hydrolyzed and condensed, which decreased the possibility of the self-condensation of triethoxysilane to form the silica encapsulated small aggregates of several MNPs. The mechanism of this reaction could be described as follows: under the catalyst of TEA, BTPAm first replaced the OA and hydrolyzed to silanol group by the water absorbed on the surface of MNPs. Then the silanol groups condensed with the hydroxyl group on the surface of MNPs or self-condensed with each other to form a Si–O–Si network on the surface of MNPs.

3.4. Surface initiated ATRP of styrene

The initiator-coated MNPs were subsequently used for the copper-mediated ATRP of styrene without free initiators (Scheme 1). The surface initiated ATRP of styrene exhibited the characteristics of a controlled/"living" polymerization. The

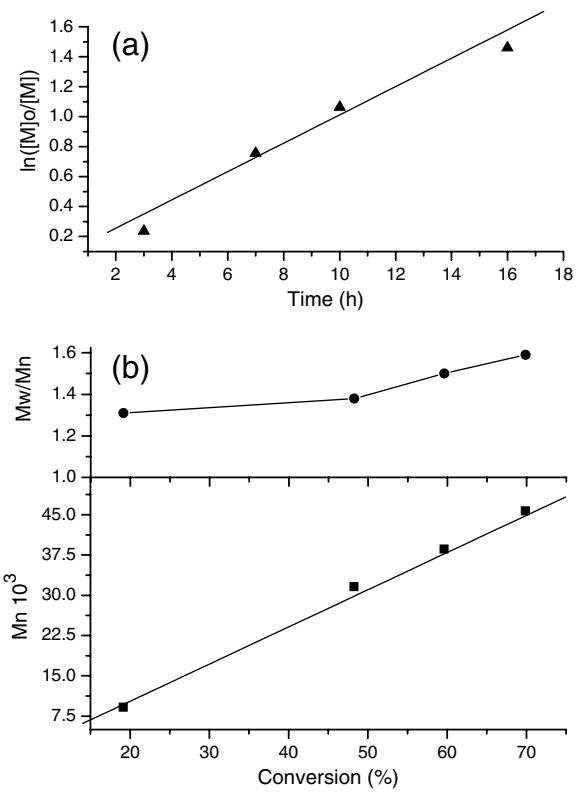

Fig. 5. (a) Plot of $\ln([M]_0/[M])$ versus time for the surface initiated ATRP of PS and (b) evolution of M_n and M_w/M_n of PS as a function of monomer conversion.

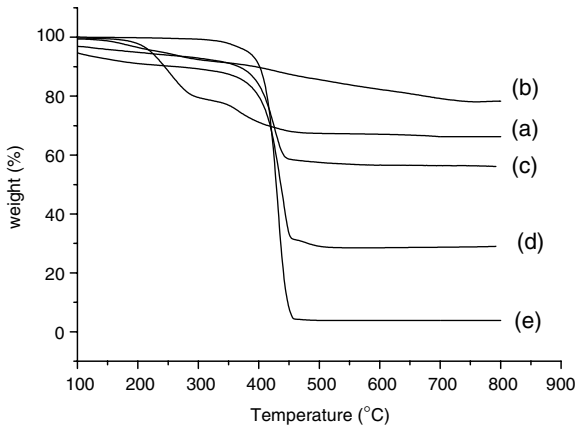

Fig. 6. TGA curves of (a) OA coated MNPs, (b) BTPAm modified MNPs, and (c, d, and e) PS coated MNPs after polymerization time of 0.5 h, 3 h, and 16 h, respectively.

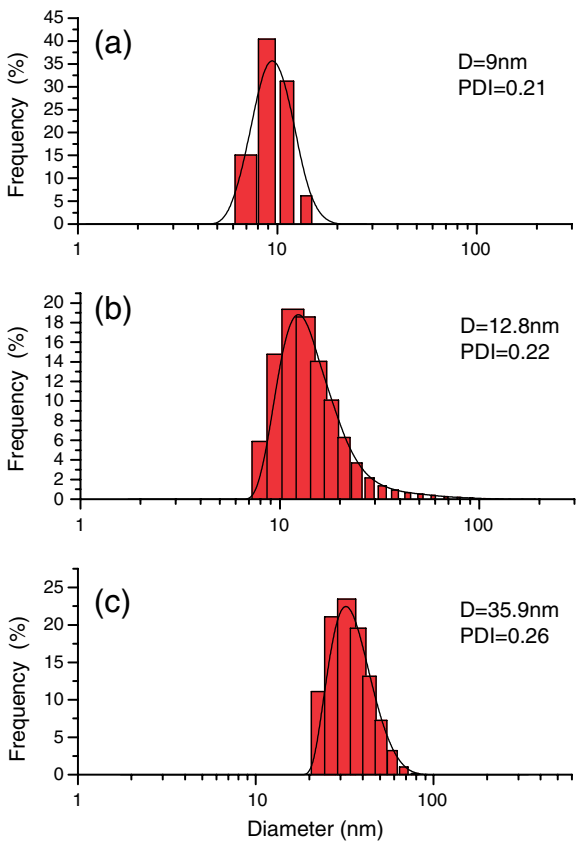

Fig. 7. Size distribution of (a) OA coated MNPs in toluene, (b) BTPAm modified MNPs in toluene and (c) PS coated MNPs in toluene ($M_n = 46{,}100$), as estimated by DLS, determined by histogram fit.

first-order kinetic plot of monomer conversion for the solution polymerization of PS is shown in Fig. 5a. The plot can be approximated by a straight line, thus giving first-order kinetics with respect to monomer conversion. The linear relationship reveals that the concentration of the propagating species is constant throughout the course of polymerization. Fig. 5b shows the evolution of M_n and the M_w/M_n of the produced polymer as a function of monomer conversion. The M_n value increases linearly with increasing monomer conversion. All these results confirm that the surface initiated ATRP of PS proceeds in a living fashion.

TGA studies were carried out to determine the graft density for MNPs coated by OA, BTPAm, and PS. MNPs after each stage of modification give their distinctive TGA curves, which provide indications of the amount of OA, initiator and PS on MNPs. TGA curve of OA coated MNPs (Fig. 6a) shows a weight loss of about 32.7%, which is higher than that of previous work because of the presence of ''free'' OA. Considering the SiO_2 ash remained in the residue after oxidation of the initiator molecule and it is estimated that the initiator graft density of BTPAm-immobilized MNPs is about 6.3 molecules per nm^2, which is similar with the result of 6.4 molecules per nm^2 by element analysis. The high graft density of initiators on the surface of MNPs provides PS more sites to graft from. However, the graft density of PS on the surface of MNPs calculated from TGA is only 0.38 molecules per nm^2. The similar result is found in the previous work [2]. As shown in Fig. 6c–e, the amount of polymer on MNPs surface increases with polymerization time. The weight loss of PS-immobilized MNPs is 33% (100–800 °C) (0.24 molecules per nm^2) after 0.5 h polymerization and increases to 71% (0.25 molecules per nm^2) after 3 h polymerization. With a 16 h polymerization time, the weight loss of PS-immobilized MNPs is 95% (0.38 molecules per nm^2). It is obviously that the graft density of PS on the surface of MNPs increases from 0.24 molecules per nm^2 at early stage of polymerization to 0.38 molecules pre nm^2 of final products. This is because that in the final

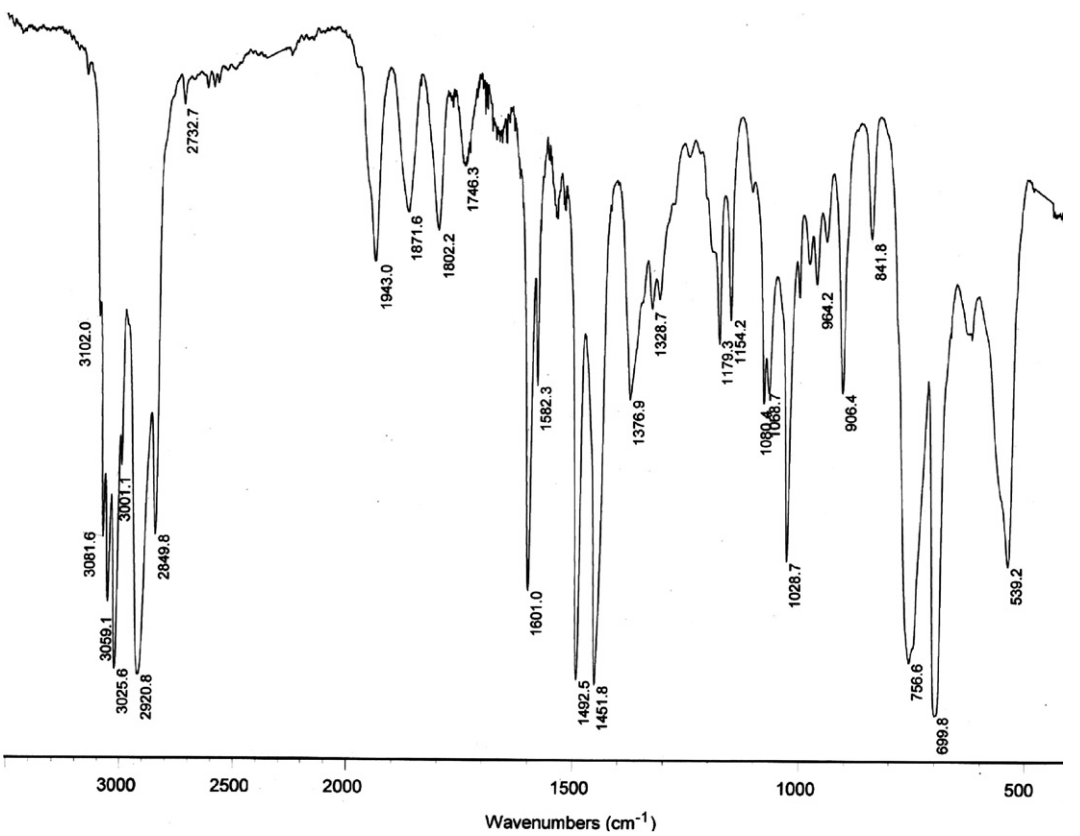

Fig. 8. IR spectrum of the PS coated Fe_3O_4 MNPs.

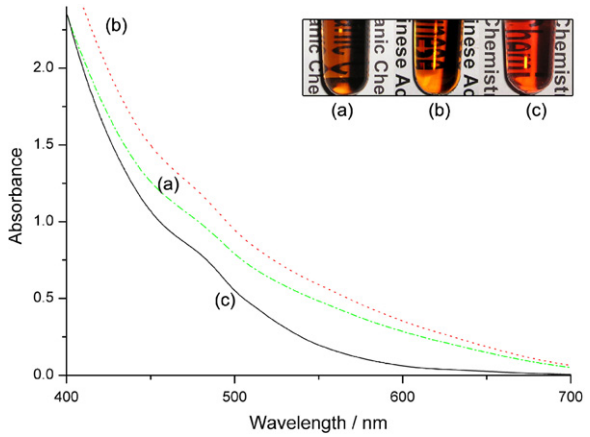

Fig. 9. UV spectrums of the MNPs: (a) OA coated; (b) BTPAm modified and (c) PS coated.

stage of the polymerization, more thermo-initiated ungrafted PS chains come into being due to the absence of the free initiators. And it is also confirmed by the fact that the ratio of M_w/M_n increases during the polymerization (Fig. 5).

After surface coated with PS, MNPs could be well dispersed in toluene, THF etc. As shown in Fig. 7, the hydrodynamic size of OA coated, BTPAm modified and PS-immobilized MNPs measured to be 9.1 nm, 12.8 nm and 35.9 nm is well agree to the result of TEM analysis, which confirms that there is minimal aggregation during the whole process of modification.

Fig. 8 shows representative FT–IR spectroscopy of the core/shell nanoparticles. The observed strong IR absorption bands at 3030–2800 cm^{-1}, 1600 cm^{-1}, 1400–1000 cm^{-1}, and 700 cm^{-1} agree well with the PS standard. The UV–vis absorption of PS grafted nanoparticles is shown in Fig. 9c. Fig. 9a and b are the spectrum of OA coated and initiator modified MNPs. They are all brownish transparent dispersion and have broad absorption peaks at 470 nm that come from iron oxide [15]. XPS analysis was carried out to determine the surface composition of PS coated MNPs. As shown in Fig. 3e, one prominent photoelectron lines at binding energy of about 285 eV, which is attributed to C1s, is observed in the wide scan spectrum. The absence of the signals for Fe, Si, N and Br indicates that PS shell covers MNPs completely. The C1s core-level spectrum also confirms the well coverage of PS shell on MNPs. Only one peak at about 284.8 eV is observed, which is attributed to *C*–C and *C*–H (Fig. 3f).

4. Conclusions

In conclusion, the initiators for ATRP have been immobilized on the surface of MNPs without any aggregates through our novel approach, which is the combination of ligand exchange and condensation of BTPAm. From the as-synthesized macroinitiators, the polymer hybrid MNPs with a well-defined, covalently bonded PS shell have been successfully prepared through the surface initiated ATRP, which exhibits a characteristic of a controlled/"living" polymerization. Because of the covalent bonds between PS chains and MNPs, it is possible to avoid the PS shell being exchanged by other ligands or washed away. This novel approach to immobilize ATRP initiators and "graft from" method of ATRP should be able to be used in the synthesis of other polymer coated MNPs with increasing complexity and functionality in the polymeric shell.

Acknowledgement

This work was financial supported by the National Nature Science Foundation of China (50573080).

Appendix A. Supplementary data

Supplementary data associated with this article can be found, in the online version, at doi:10.1016/j.eurpolymj.2006.10.021.

References

[1] Matyjaszewski K, Xia J. Chem Rev 2001;101:2921.
[2] (a) Kohji O, Takashi M, Kyoungmoo K. Macromolecules 2005;38:2137–42;
(b) Li D, Jones GL, Dunlap JR, Hua F, Zhao B. Langmuir 2006;22:3344–51.
[3] Mandal TK, Fleming MS, Walt DR. Nano Letters 2002; 2(1):3–7.
[4] Christy R, Vestal Z, Zhang J. J Am Chem Soc 2002; 124:14312–3.
[5] (a) Wang Y, Teng X, Wang J, Yang H. Nano Letters 2003;3(6):789–93;
(b) Gravano SM, Dumas R, Liu K, Patten TE. J Polym Sci A: Polym Chem 2005;43:3675–88.
[6] Patten TE, Matyjaszewski K. Adv Mater 1998;10:901.
[7] Li G, Fan J, Jiang R, Gao Y. Chem Mater 2004;16:1835–7.
[8] (a) Hu F, Neoh KG, Cen L, Kang ET. Biomacromolecules 2006;7:809–16;
(b) Marutani E, Yamamoto S, Ninjbadgar T, Tsujii Y, Fukuda T, Takano M. Polymer 2004;45:2231–5;
(c) Ninjbadgar T, Yamamoto S, Fukuda T. Solid State Sci 2004;6:879–85.

[9] Sun Y, Ding X, Zheng Z, Cheng X, Hu X, Peng Y. Chem. Commun 2006(26):2765–7.
[10] Wang W, Efrima S, Regev O. Langmuir 1998;14:602–10.
[11] Wu N, Fu L, Su M, Asiam M, Wong K, Dravid VP. Nano Letters 2004;4(2):383–6.
[12] Pluddemann EP. Silane coupling agents. New York: Plenum Press; 1982.
[13] (a) Deng Y, Wang C, Fu S. Colloids Surface A: Physicochem. Eng. Aspects 2005;262:73–87;
(b) Yamaura M, Camilo RL, Sampaio LC, Toma HE. J Magn Magn Mater 2004;279:210–7.
[14] (a) Bourlinos AB, Bakandritsos A, Georgakilas V, Petridis D. Chem Mater 2002;14:3226–8;
(b) Kim M, Chen Y, Liu Y, Peng X. Adv Mater 2005;17:1429–32.
[15] Cornell RM, Schwertmann U. The iron oxides: structure, properties, reactions, occurrence and uses. Weinheim: VCH; 1996.